THE JOURNAL OF BIOLOGICAL CHEMISTRY VOL. 287, NO. 42, pp. 35153–35160, October 12, 2012

Inactivation of Pyruvate Dehydrogenase Kinase 2 by Mitochondrial Reactive Oxygen Species*[S]

Received for publication, July 11, 2012, and in revised form, August 17, 2012 Published, JBC Papers in Press, August 21, 2012, DOI 10.1074/jbc.M112.400002

Thomas R. Hurd[1,2], **Yvonne Collins**[1], **Irina Abakumova**[3], **Edward T. Chouchani, Bartlomiej Baranowski**[4], **Ian M. Fearnley, Tracy A. Prime, Michael P. Murphy**[5], **and Andrew M. James**

From the Mitochondrial Biology Unit, Medical Research Council, Cambridge CB2 0XY, United Kingdom

Background: Reactive oxygen species (ROS) can potentially regulate metabolism, but the targets are unclear.
Results: Mitochondrial ROS oxidize cysteines on pyruvate dehydrogenase kinase 2 (PDHK2), leading to pyruvate dehydrogenase complex activation.
Conclusion: Inactivation of PDHK2 by ROS suggests how the redox regulation of metabolism may occur.
Significance: This finding indicates a novel pathway through which mitochondrial ROS may alter metabolism.

Reactive oxygen species are byproducts of mitochondrial respiration and thus potential regulators of mitochondrial function. Pyruvate dehydrogenase kinase 2 (PDHK2) inhibits the pyruvate dehydrogenase complex, thereby regulating entry of carbohydrates into the tricarboxylic acid (TCA) cycle. Here we show that PDHK2 activity is inhibited by low levels of hydrogen peroxide (H_2O_2) generated by the respiratory chain. This occurs via reversible oxidation of cysteine residues 45 and 392 on PDHK2 and results in increased pyruvate dehydrogenase complex activity. H_2O_2 derives from superoxide ($O_2^{\cdot-}$), and we show that conditions that inhibit PDHK2 also inactivate the TCA cycle enzyme, aconitase. These findings suggest that under conditions of high mitochondrial $O_2^{\cdot-}$ production, such as may occur under nutrient excess and low ATP demand, the increase in $O_2^{\cdot-}$ and H_2O_2 may provide feedback signals to modulate mitochondrial metabolism.

Mitochondrial ROS[6] production is sensitive to membrane potential and the redox state of the electron carriers NADH and coenzyme Q (1). Consequently, redox changes to mitochondrial proteins in response to the ROS, superoxide ($O_2^{\cdot-}$), and hydrogen peroxide (H_2O_2) could coordinate mitochondrial function upon changes in substrate supply, ATP demand, proton leak, calcium uptake, or oxygen concentration (1, 2). $O_2^{\cdot-}$ can directly inactivate iron-sulfur center proteins and is converted to H_2O_2 by manganese superoxide dismutase (1, 3). Subsequently, H_2O_2 reversibly modifies protein activity by altering the redox state of responsive cysteine residues (2, 4, 5). H_2O_2 modifies target cysteine thiols directly to form a sulfenic acid or indirectly, via peroxiredoxins or through the glutathione (GSH) or thioredoxin pools (2, 5). ROS signals are also generated by NADPH oxidases through activation of cell surface receptors such as those for angiotensin II, tumor necrosis factor-α, or insulin (4, 6, 7).

To identify sites of mitochondrial redox regulation by H_2O_2, we developed a proteomic technique, redox-difference gel electrophoresis, to screen for mitochondrial thiol proteins that reacted with physiologically plausible levels of H_2O_2 (3). A small group of proteins was consistently modified by 2.5 μM H_2O_2 or by a similar level of endogenous H_2O_2 produced by reverse electron transport (RET) at complex I (3). Within this group was pyruvate dehydrogenase kinase 2 (PDHK2), a major regulator of the pyruvate dehydrogenase complex (PDC) (3, 8). PDC is comprised of three enzymes, pyruvate dehydrogenase (PDH, E1), dihydrolipoamide acetyltransferase (E2), and dihydrolipoamide dehydrogenase (E3), which catalyze the conversion of pyruvate to acetyl-CoA. Thus PDC activity dictates the rate of entry of pyruvate into the TCA cycle and subsequently to oxidative phosphorylation or fatty acid synthesis (9). PDC activity is primarily regulated through phosphorylation (inactivation) and dephosphorylation (activation) of PDH on serine residues 293, 300, and 232 of the E1α subunit (10). Phosphorylation of any of these sites leads to PDC inhibition (8), and in mammals, phosphorylation is regulated by four PDHK isoforms and two phosphatases (9, 11, 12). PDHK2 is the ubiquitously expressed form of PDHK and is thought to exert short-term control over PDC activity.

Our finding of redox active thiols on PDHK2 suggested that redox regulation of PDHK2 activity could control pyruvate entry into the TCA cycle. Here we investigated whether H_2O_2-induced thiol modifications on PDHK2 regulate PDC and affect mitochondrial carbohydrate metabolism. We found that low micromolar concentrations of H_2O_2 inhibit PDHK2 activity by

* This work was supported by the Medical Research Council (United Kingdom).
[S] This article contains supplemental Materials and Methods and Figs. S1–S8.
[1] Both authors contributed equally to this work.
[2] Present address: Dept. of Cell Biology, Howard Hughes Medical Institute (HHMI) and Kimmel Center for Biology and Medicine of the Skirball Institute, New York University School of Medicine, New York, NY 10016.
[3] Present address: Pathology Dept., Institute of Neuropathology, University Hospital Zurich, Schmelzbergstrasse 12, 8091 Zurich, Switzerland.
[4] Present address: UCL Cancer Institute and Samantha Dickson Brain Cancer Unit, University College London, Paul O'Gorman Bldg., Gower St., London WC1E 6BT, United Kingdom.
[5] To whom correspondence should be addressed: Medical Research Council (MRC) Mitochondrial Biology Unit, Wellcome Trust/MRC Building, Hills Rd., Cambridge CB2 0XY, United Kingdom. Tel.: 44-1223-252900; Fax: 44-1223-252905; E-mail: mpm@mrc-mbu.cam.ac.uk.
[6] The abbreviations used are: ROS, reactive oxygen species; DCA, dichloroacetic acid; FCCP, carbonyl cyanide 4-(trifluoromethoxy)phenylhydrazone; NEM, *N*-ethyl maleimide; Mal-PEG, maleimide conjugated to PEG; PDC, pyruvate dehydrogenase complex; PDH, pyruvate dehydrogenase; PDHK, pyruvate dehydrogenase kinase; ET, reverse electron transport; TCA, tricarboxylic acid.

modification of cysteine residues 45 and 392, thereby decreasing PDC phosphorylation and increasing flux through PDC. The same low levels of ROS also inactivated aconitase, suggesting that mitochondrial ROS can modulate several sites of mitochondrial carbohydrate metabolism.

EXPERIMENTAL PROCEDURES

Mitochondrial Preparations and Incubations—Rat heart mitochondria were prepared by homogenization in STEB (250 mM sucrose, 5 mM Tris-HCl, 1 mM EGTA, 0.1% fatty acid free BSA, pH 7.4) using an ULTRA-TURRAX blender followed by differential centrifugation (3). Unless otherwise stated, incubations were at 1 mg of mitochondrial protein × ml^{-1} at 37 °C with gentle agitation in SHE (250 mM sucrose, 40 mM HEPES, 1 mM EGTA, pH 7.4) with 5 mM glutamate/5 mM malate. RET was induced by incubating in SHEB (SHE with 0.01% fatty acid free BSA) and 10 mM succinate as substrate. RET was prevented either by adding 4 μg × ml^{-1} rotenone or 400 nM carbonyl cyanide 4-(trifluoromethoxy)phenylhydrazone (FCCP) or by omitting BSA. Additional details are available in the supplemental material.

Creation of PDHK2 Mutations—Homo sapiens PDHK2 including its N-terminal mitochondrial targeting sequence was amplified by PCR from an Mammalian Genome Collection clone (Open Biosystems, MHS1011-9199126) (Table S2). PCR products were digested and ligated into a pcDNA5/FRT/TO vector containing C-terminal FLAG and STREP2 tags. Cysteine to alanine point mutations were then generated before transfection into HEK293 cells (Flp-In™-293, Invitrogen) by electroporation. PDHK2 was overexpressed using doxycycline and a tetracycline-inducible system from Invitrogen (Flp-In™ T-REx™). HEK293 cells were cultured at 37 °C in DMEM in a humidified atmosphere of 95% air, 5% CO_2. 24 h prior to measurement of PDC phosphorylation or cellular respiration, pyruvate was omitted from the culture medium unless otherwise indicated. Additional details are available in the supplemental material.

PDHK2 and Aconitase Measurements—PDHK2 redox state was measured by blocking reduced thiols with *N*-ethylmaleimide (NEM), reducing oxidized thiols with dithiothreitol (DTT), and alkylating them with maleimide conjugated to a polyethylene glycol polymer (Mal-PEG) (Iris Biotech GmbH) according to Fig. 1*A* (13). Samples were analyzed by immunoblotting. An antibody against PDHK2 (AP7039b, Abgent) was used to detect PDHK2 in heart mitochondria, and an anti-FLAG antibody (mouse monoclonal, Sigma F1804) was used to detect FLAG-tagged PDHK2 in HEK293 cells. Isolated, purified PDHK2 was detected by Coomassie Blue staining of polyacrylamide gels (Table S1). PDHK activity was assessed from the initial rate of [^{32}P]phosphate incorporation from [γ-^{32}P]ATP into exogenous porcine PDC. PDC phosphorylation was assessed by immunoblotting using Calbiochem® antibodies specific for PDC phosphorylated on Ser-232 (Site 3) (AP1063), Ser-293 (Site 1) (AP1062), and Ser-300 (Site 2) (AP1064) of the E1α subunit (14). Total PDC was determined using an antibody against the E1α subunit (A-21323, Sigma). Aconitase activity was measured as described previously (15). Additional details are available in the supplemental material.

Respiration Measurements—Isolated rat heart mitochondria (0.5 mg × ml^{-1}) were incubated in SHEB with 10 mM succinate to induce RET. RET was prevented in parallel incubations by including 400 nM FCCP or by omitting BSA. After 5 min, 20 mM malonate was added to prevent further succinate oxidation, along with FCCP if not already present. Uncoupled respiration was then measured at 37 °C using an oxygen electrode (Rank Brothers Ltd., Bottisham, Cambridge, UK) after the addition of 10 mM glutamate/malate or 10 mM pyruvate.

PDHK2-overexpressing cell lines were incubated until ~80% confluency in 24-well Seahorse plates coated with poly-D-lysine before the addition of 50 ng × ml^{-1} doxycycline for 24 h. Culture medium was replaced with Seahorse assay buffer (3.5 mM KCl, 120 mM NaCl, 1.8 mM $CaCl_2$, 0.4 mM KH_2PO_4, 1.2 mM Na_2SO_4, 20 mM Hepes, 2 mM Mg_2SO_4, 0.4% (w/v) BSA, pH 7.4) containing 15 mM glucose and 50 ng × ml^{-1} doxycycline and incubated for 1 h at 37 °C. Cellular oxygen consumption was measured using a Seahorse XF24 extracellular flux analyzer (Seahorse Bioscience). Four initial measurement cycles were taken to equilibrate the plate followed by eight measurement cycles with no addition, H_2O_2, or dichloroacetic acid (DCA). This was followed by four measurement cycles with 4 μg × ml^{-1} rotenone and 10 μM antimycin to inhibit mitochondrial respiration. Additional details are available in the supplemental material.

RESULTS

H_2O_2 Reversibly Oxidizes Thiols on PDHK2 within Isolated Mitochondria—A proteomic screen of heart mitochondria for proteins sensitive to H_2O_2 suggested that PDHK2 has at least one thiol that is modified by low levels of H_2O_2 (3). PDHK2 has four cysteine residues, so we developed an immunoblotting procedure to visualize the number and ratio of reduced to oxidized thiols on PDHK2 (Fig. 1*A*) (13). We exposed isolated mitochondria to the redox cycler menadione (Fig. 1*B*), which continually generates mitochondrial $O_2^{\cdot-}$ that dismutates to H_2O_2 (16), or to bolus H_2O_2 (Fig. 1*C*). In the absence of oxidant, PDHK2 was largely in a reduced form (Fig. 1, *B* and *C*) of identical molecular weight to PDHK2 treated with just NEM (supplemental Fig. S1). Exposure to menadione, or to H_2O_2 itself, led to dose-dependent loss of reduced PDHK2 and formation of a higher molecular weight oxidized form of PDHK2 (Fig. 1, *B* and *C*). Importantly, physiologically plausible concentrations of H_2O_2, produced without inhibitors via RET at complex I (1), also led to ~25% oxidation of PDHK2 (Fig. 1*D*). For thiol oxidation to regulate PDHK2, it should be readily reversed once the H_2O_2 concentration returns to basal levels. Mitochondria were incubated with 25 μM H_2O_2, and PDHK2 redox state was measured as the H_2O_2 was metabolized (Fig. 1*E*). After 10–15 min, PDHK2 had largely returned to its reduced state (Fig. 1*E*), correlating with the rate of mitochondria-mediated H_2O_2 degradation (2.4 ± 0.3 μM H_2O_2/min/mg of protein, $n = 3$ mean ± S.D.). In contrast, oxidation of PDHK2 by menadione was not reversed, consistent with its continual production of H_2O_2 (Fig. 1*F*). Analogous experiments were carried out on PDHK1, PDHK3, and PDHK4 (12), and only PDHK1 contained thiols that were oxidized by H_2O_2 (supplemental Fig. S2). As PDHK2

is responsible for short-term metabolic responses, we focused on it.

The concentrations of H_2O_2 used had no effect on general mitochondrial protein thiols (3) or the mitochondrial GSH pool (supplemental Fig. S3*A*). However, thioredoxin 2 and peroxiredoxin III are particularly sensitive to oxidation, and both were partially oxidized by the low levels of H_2O_2 (supplemental Fig. S3, *B* and *C*) (17). Thus the concentration of H_2O_2 capable of reversibly oxidizing PDHK2 does affect other redox-sensitive proteins, but does not generally oxidize mitochondrial thiols.

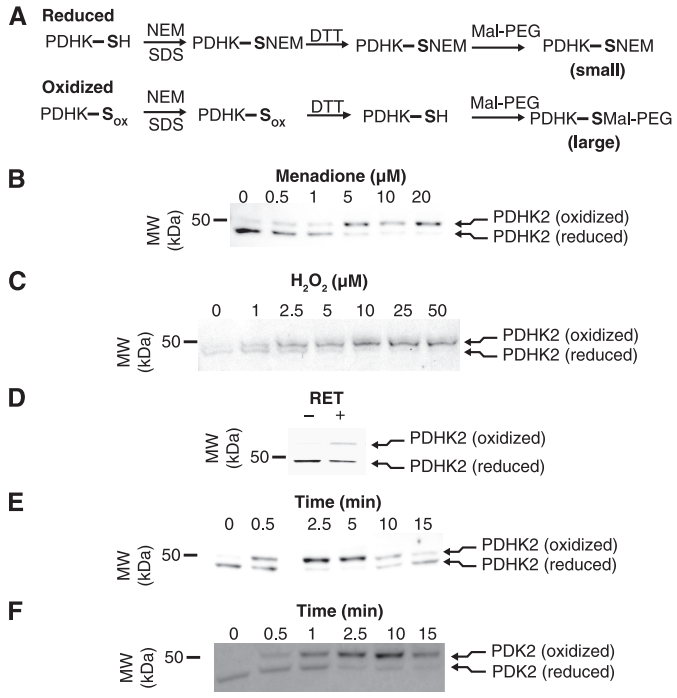

FIGURE 1. **PDHK2 thiols were reversibly oxidized in isolated rat heart mitochondria by low concentrations of H_2O_2.** *A*, measurement of PDHK2 redox state. Mitochondria were treated with SDS and NEM to derivatize all reduced thiols. NEM was removed, and oxidized thiols were reduced with DTT and reacted with maleimide conjugated to a 2- or 5-kDa polyethylene glycol polymer (Mal-PEG). PDHK2 was assessed by SDS-PAGE and immunoblotting with a PDHK2 specific antibody. *B* and *C*, low levels of menadione or H_2O_2 oxidize PDHK2 thiols. Mitochondria were incubated with menadione or H_2O_2 for 1 min. *MW*, molecular mass markers. *D*, RET oxidizes PDHK2 thiols. Mitochondria were exposed to RET for 5 min. *E*, PDHK2 is reversibly oxidized by H_2O_2. Mitochondria were treated with 25 μM H_2O_2. *F*, PDHK2 is persistently oxidized by menadione. Mitochondria were treated with 5 μM menadione.

H_2O_2 Decreases PDHK2 Activity in Mitochondria and Cells—To determine whether thiol oxidation on PDHK2 affected its kinase activity, we incubated mitochondria with H_2O_2, then prevented further kinase and phosphatase activity by lysing them with sodium dodecyl sulfate (SDS), and used a phosphorylation-specific antibody that only detects phosphorylation of Ser-293 (Site 1) of the E1α subunit of PDH (Fig. 2*A*) (10, 14). In mitochondria, Ser-293 (Site 1) was phosphorylated, and incubation with H_2O_2 largely abolished this (Fig. 2*A*). To show that stimulation of PDC phosphatases was not responsible for the loss of PDC phosphorylation, mitochondria were lysed with Triton X-100 in the presence of the phosphatase inhibitor, NaF (Fig. 2*B*) (18). Inclusion of NaF did not prevent these lysates from incorporating [^{32}P]phosphate from [γ-^{32}P]ATP into purified porcine PDH in an H_2O_2-sensitive manner (Fig. 2*B*). This shows that redox regulation is not phosphatase-dependent. To see whether H_2O_2 also decreased PDHK2 activity in intact cells, we lysed them in SDS and assessed phosphorylation of Ser-293 (Site 1) on the E1α subunit of PDC as in Fig. 2*A* (Fig. 2, *C* and *D*). In HEK293 cells, PDC was phosphorylated, and this was abolished by the PDHK inhibitor DCA (Fig. 2, *C* and *D*) (19, 20). PDC phosphorylation also decreased with low concentrations of H_2O_2 for 5 min (Fig. 2*C*), and this gradually recovered after 30 min (Fig. 2*D*). The decrease in PDC phosphorylation in mitochondria and cells exposed to H_2O_2 is consistent with the reversible oxidation of thiols on PDHK2 affecting the phosphorylation status and activity of PDC.

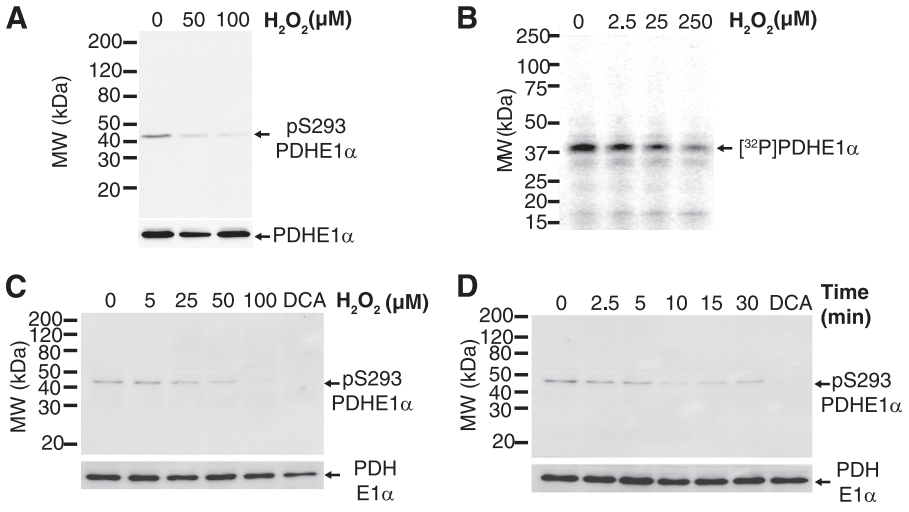

FIGURE 2. **H_2O_2 decreased PDC phosphorylation by inhibiting PDHK2 in mitochondria and in cells.** *A*, phosphorylation of PDC was decreased in H_2O_2-treated mitochondria. Mitochondria were incubated with H_2O_2 and lysed in SDS, and PDC phosphorylation was assessed using an antibody against the PDH E1α subunit of PDC phosphorylated on Ser-293 (*pS293*) (Site 1) (14). The blot was reprobed with an antibody to all forms of PDH E1α. *MW*, molecular mass markers. *B*, H_2O_2-sensitive phosphorylation of PDC is not mediated by phosphatases. Mitochondria were treated with H_2O_2 for 5 min, and the ability of NaF-inhibited Triton X-100 lysates to incorporate [^{32}P]phosphate into purified porcine PDC was then measured by phosphorimaging. *C*, PDC phosphorylation was decreased in H_2O_2-treated cells. HEK293 cells were incubated with H_2O_2 for 5 min and lysed in SDS, and PDH E1α phosphorylation was assessed. *D*, PDC phosphorylation was reversible in H_2O_2-treated cells. HEK293 cells were exposed to 25 μM H_2O_2, and PDH E1α phosphorylation was assessed subsequently.

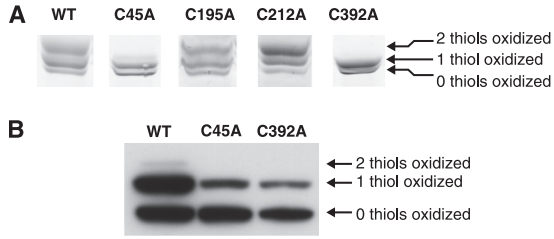

FIGURE 3. **Both Cys-45 and Cys-392 on PDHK2 could be oxidized.** *A*, purified WT PDHK2 contained two cysteines that spontaneously oxidize. Purified His-tagged WT or mutant versions of PDHK2 were incubated without reductant. Redox forms were separated as in Fig. 1*A* and then visualized by Coomassie Blue staining of SDS-PAGE gels. *B*, H_2O_2 could oxidize both Cys-45 and Cys-392 in cells. Cells overexpressing WT or mutant FLAG-tagged PDHK2 were incubated with 100 μM H_2O_2 and then prepared as in Fig. 1*A* before SDS-PAGE and immunoblotting with anti-FLAG.

Cys-45 and Cys-392 Are the Redox-sensitive Cysteine Residues on PDHK2—PDHK2 has four cysteine residues: Cys-45, Cys-195, Cys-212, and Cys-392 numbered according to the mature rat PDHK2 sequence (21). Despite no known function, all are conserved in PDHK2 in mammals and zebrafish, whereas three (Cys-45, Cys-195, and Cys-212) are conserved in *Drosophila* homolog PDHKA (supplemental Fig. S4). In mammals, all four PDHK2 cysteine residues are conserved on PDHK1 and PDHK4, whereas three of the four (Cys-45, Cys-195 and Cys-212) are conserved on PDHK3 (supplemental Fig. S5). To identify the cysteine residues oxidized by H_2O_2, we replaced each cysteine with an alanine to make five recombinant versions of PDHK2: wild-type (WT), C45A, C195A, C212A, and C395A. After expression in *Escherichia coli* and isolation, we measured the number of thiols oxidized on WT PDHK2 *in vitro*. Purified WT, C195A, and C212A PDHK2 spontaneously gave three redox forms corresponding to oxidation of zero, one, and two cysteine residues (Fig. 3*A*). When Cys-45 or Cys-392 was replaced, the PDHK2 band with two oxidized cysteine residues was lost (Fig. 3*A*). Thus *in vitro*, the oxidizable thiols of PDHK2 are those of Cys-45 and Cys-392.

The WT, C45A, and C392A forms of PDHK2 were overexpressed in HEK293 cells under a tetracycline-inducible system allowing recombinant protein to dilute out endogenous PDHK over 24 h prior to the experiment (supplemental Fig. S6, *A* and *B*). Some constructs contained a C-terminal FLAG tag to facilitate detection on immunoblots. All possible thiol redox states of PDHK2 could be seen when cell extracts were reduced with DTT and incubated with a range of ratios of NEM and Mal-PEG (supplemental Fig. S7*A*). Incubation with either NEM or Mal-PEG alone led to one PDHK2 band, whereas intermediate NEM/Mal-PEG ratios led to five distinct bands. Combined samples were used as standards to show that in cells, all four thiols of WT PDHK2 were largely reduced under control conditions (supplemental Fig. S7*B*). When cells were exposed to bolus H_2O_2 (Fig. 3*B*) or persistent levels of H_2O_2 via menadione (supplemental Fig. S7*B*), PDHK2 became oxidized on one or two cysteines. In the absence of either Cys-45 or Cys-392, oxidation of PDHK2 decreased, and neither form had two oxidized thiols (Fig. 3*B*). Thus in cells, PDHK2 is largely reduced but is sensitive to oxidation on both Cys-45 and Cys-392.

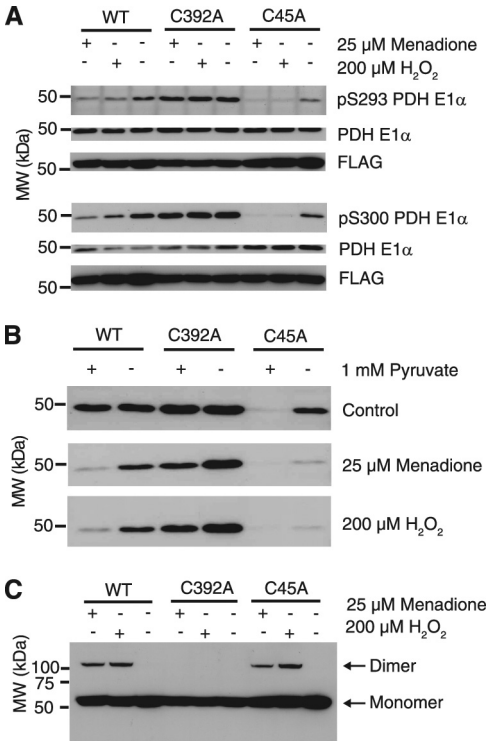

FIGURE 4. **Oxidation of Cys-45 or Cys-392 inhibited PDHK2 activity.** *A*, oxidation of Cys-392 inhibited PDC phosphorylation in the absence of pyruvate. Cells overexpressing FLAG-tagged WT or mutant PDHK2 were incubated with 200 μM H_2O_2 or 25 μM menadione for 5 min. Cells were lysed before SDS-PAGE and immunoblotting against Ser-293 (Site 1) or Ser-300 (Site 2)-phosphorylated PDHE1α. Membranes were reprobed with anti-FLAG and then anti-PDHE 1α. *MW*, molecular mass markers; *pS293*, phosphorylated Ser-293. *B*, PDHK2 conformation affected its sensitivity to oxidation. Cells overexpressing FLAG-tagged WT or mutant PDHK2 were grown $\pm$ 1 mM pyruvate for 24 h. They were then incubated $\pm$ 1 mM pyruvate and 200 μM H_2O_2 or 25 μM menadione for 5 min. Cells were lysed before SDS-PAGE and immunoblotting against Ser-300 (Site 2)-phosphorylated PDH E1α (*pS300*). *C*, oxidation leads to an interprotein disulfide in WT and C45A PDHK2 not found in the C392A mutant. Cells overexpressing WT or mutant PDHK2 were incubated with 200 μM H_2O_2 or 25 μM menadione for 5 min. Cells were lysed in the presence of NEM before nonreducing SDS-PAGE and immunoblotting with anti-FLAG.

Mutation of Cys-45 or Cys-392 to Alanine Affects PDHK2 Activity in Cells—We next assessed whether C45A or C392A PDHK2 mutations affected phosphorylation of Ser-293 (Site 1) and Ser-300 (Site 2) of PDH E1α (Fig. 4). Cells expressing WT PDHK2 could phosphorylate both Ser-293 (Site 1) and Ser-300 (Site 2) of PDH E1α, and this could be inhibited by H_2O_2 or menadione (Fig. 4*A*). Cells expressing the C392A form of PDHK2 also phosphorylated Ser-293 (Site 1) and Ser-300 (Site 2) of PDH E1α, but this phosphorylation was largely insensitive to H_2O_2 or menadione (Fig. 4*A*). When Cys-45 was mutated to alanine, the phosphorylation of Ser-293 (Site 1) and Ser-300 (Site 2) of PDH E1α was weak even in the absence of oxidant (Fig. 4*A*). Phosphorylation of both Ser-293 (Site 1) and Ser-300 (Site 2) of PDH E1α was abolished by H_2O_2 or menadione in cells expressing C45A PDHK2. This suggests that oxidation of Cys-392 is responsible for redox inactivation of PDHK2, whereas Cys-45 is critical for maximal PDHK2 activity. The changes in phosphorylation do not result from differences in the amount of PDH E1α or PDHK2 (Fig. 4*A*).

PDHK2 has been crystallized in three structural forms and is activated by the L2 domain of PDC, NADH, and acetyl-CoA

and inactivated by pyruvate and ADP (9, 11). Cysteine reactivity is dependent on the local environment around the thiol, so to see whether PDHK2 conformation affected sensitivity to oxidation, this experiment was repeated in medium with pyruvate (Fig. 4*B*). This should favor conformations not bound to the L2 domain of PDC. In the presence of pyruvate, Cys-45 appeared essential for kinase activity as the C45A mutant did not phosphorylate PDH E1α even in the absence of oxidant. In contrast, pyruvate had little effect on WT or C392A PDHK2 under the same conditions. Finally, pyruvate resulted in the C392A mutant becoming sensitive to either H_2O_2 or menadione, implying that Cys-45 is also redox-sensitive in some situations (Fig. 4*B*). These results suggest that the reactivity of Cys-45 and Cys-392 may vary between the three structural forms.

PDHK2 Can Form a Dimer under Oxidizing Conditions—Nonreducing denaturing electrophoresis of isolated PDHK2 showed that WT, C45A, C195A, and C212A PDHK2 readily form covalent intermolecular dimers, with dimerization of C392A PDHK2 significantly less (supplemental Fig. S8*A*). Mass spectrometry showed that *in vitro*, an intermolecular disulfide between two Cys-392 residues is present (supplemental Fig. S8*B*). A higher molecular mass (~100 kDa) PDHK2-containing band, consistent with a PDHK2 homodimer, could be detected in WT and C45A cells treated with oxidant and lysed in the presence of NEM (Fig. 4*C*). This band was absent from cells carrying the C392A mutation (Fig. 4*C*). The PDHK2-containing dimer was reduced by DTT (supplemental Fig. S8*C*), indicating a disulfide. The poor correlation between dimer formation (Fig. 4*C*) and PDHK2 inactivation (Fig. 4, *A* and *B*) suggests that dimer formation is not essential for PDHK2 inactivation via Cys-392 oxidation, although it may potentiate it.

PDC Activity Changes in Response to Redox Modification of PDHK2—PDH E1α phosphorylation (Figs. 2 and 4) indicates inactive PDC, so we assessed the effect of H_2O_2 on levels of active PDC by measuring respiration. Firstly, isolated mitochondria were incubated under conditions that generate H_2O_2 via RET (3) and that modify PDHK2 (Fig. 1*D*). Mitochondria were pelleted and resuspended in buffer with pyruvate, malonate, and FCCP before transfer to an oxygen electrode. Exposure to RET increased subsequent respiration on pyruvate when compared with conditions where RET does not occur as FCCP was present throughout (Fig. 5*A*) (3). In contrast, respiration on a combination of glutamate and malate, which does not require PDC activity, was unaffected by RET (Fig. 5*A*).

Using a Seahorse extracellular flux analyzer, we measured the rate of oxygen consumption in intact cells. Inhibiting PDHK with DCA (Fig. 5*B*) showed that PDHK could affect the rate of respiration in cells metabolizing glucose. When H_2O_2 was added, it also stimulated respiration on glucose (Fig. 5*B*). H_2O_2 did not stimulate respiration in the C45A mutant under the same conditions (Fig. 5*C*), and this occurred because respiration prior to H_2O_2 addition was already high in the largely inactive C45A mutant and similar to WT PDHK2 inhibited by DCA (Fig. 5*D*). Thus inactivation of PDHK2 by DCA or the C45A mutation leads to an elevated respiration rate similar to that seen with H_2O_2 exposure. Thus PDHK2 has redox-sensitive cysteines that can be oxidized, resulting in its inactivation and increased flux through the PDC.

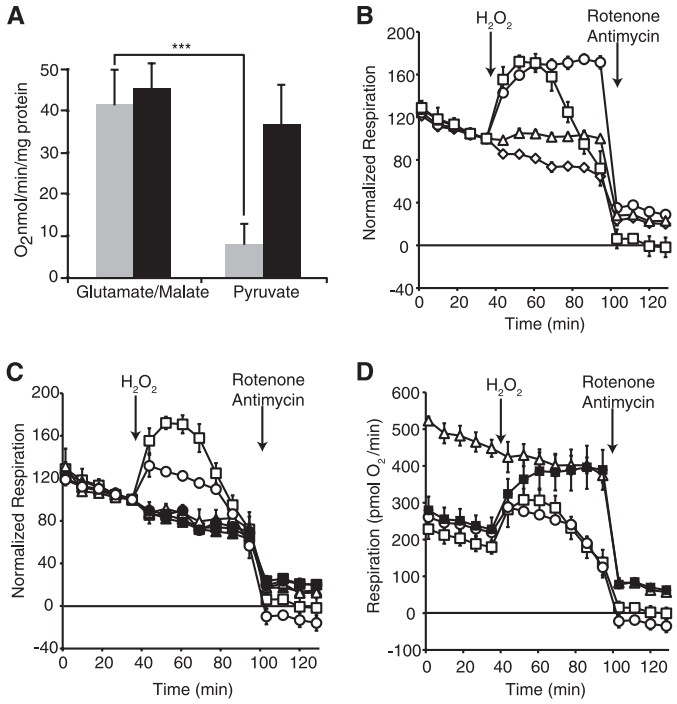

FIGURE 5. **PDC flux was sensitive to DCA, H_2O_2, and mutation of Cys-45 on PDHK2.** *A*, RET increased pyruvate oxidation. Isolated mitochondria were incubated with succinate and BSA to induce RET (3). RET was avoided by including FCCP. After 5 min, malonate was added with FCCP if it was not already present, and respiration was measured in an oxygen electrode after the addition of glutamate/malate or pyruvate. Data are ± S.D. ($n = 3$). *Black bars* are RET, and *shaded bars* are FCCP controls with no RET. ***, $p < 0.001$ compared with control by Student's *t* test. *B*, respiration is increased by DCA and H_2O_2 in cells overexpressing WT PDHK2. Oxygen consumption of cells overexpressing WT PDHK2 respiring on glucose was measured using a Seahorse flux analyzer. After four cycles, carrier (*diamonds*), 10 mM DCA (*circles*), 100 μM H_2O_2 (*triangles*), or 200 μM H_2O_2 (*squares*) were added. After a further eight cycles, rotenone and antimycin were added. Data are oxygen consumption normalized to that just prior to the addition of H_2O_2 or DCA ± S.E. ($n = 3$). *C*, respiration was not altered by H_2O_2 in cells overexpressing C45A PDHK2. Oxygen consumption of cells overexpressing WT (*squares*), C45A (*triangles*), and C392A (*circles*) PDHK2 respiring on glucose was measured. After four cycles, either carrier (*filled symbols*) or 200 μM H_2O_2 (*open symbols*) were added. After a further eight cycles, rotenone and antimycin were added. Data are oxygen consumption normalized to that just prior to the addition of H_2O_2 ± S.E. ($n = 3$). *D*, basal respiration was elevated in cells overexpressing C45A PDHK2. Oxygen consumption of cells overexpressing WT (*squares*), C45A (*triangles*), and C392A (*circles*) PDHK2 respiring on glucose was measured. After four cycles, 10 mM DCA (*filled symbols*) or 200 μM H_2O_2 (*open symbols*) was added. After a further eight cycles, rotenone and antimycin were added. Data are the rate of oxygen consumption ± S.E. ($n = 3$).

ROS Simultaneously Inactivate PDHK2 and Aconitase—H_2O_2 arises from $O_2^{\cdot-}$ dismutation, and both form when increases in membrane potential and substrate supply to the respiratory chain occur in the absence of ATP demand. Thus activating PDC in response to H_2O_2 could create a damaging feed forward loop by further increasing substrate supply to the respiratory chain. We hypothesized that this loop was prevented by redirecting substrates away from the respiratory chain via the rapid inactivation of aconitase by $O_2^{\cdot-}$ ($k = \sim 10^7$ $M^{-1} \times s^{-1}$) (22). Supporting this, we found that PDHK2 and aconitase exhibit a similar sensitivity to a titration with menadione, which generates both $O_2^{\cdot-}$ and H_2O_2 (Fig. 6*A*). Finally, physiologically relevant $O_2^{\cdot-}$ generation via RET significantly lowered aconitase activity (Fig. 6*B*). We conclude that PDHK2, like aconitase, is highly sensitive to inactivation by ROS and

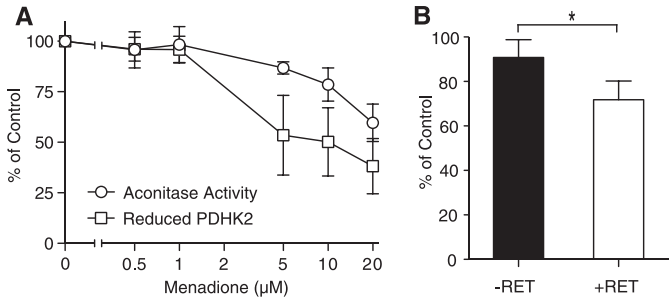

FIGURE 6. **Aconitase inactivation by mitochondrial $O_2^{\cdot-}$.** *A*, aconitase and PDHK2 were inactivated by similar concentrations of ROS. Mitochondria were exposed to menadione for 1 min before measurement of aconitase activity (*circles*) and PDHK2 redox state (the percentage of reduced to total PDHK2; *squares*). Both were normalized to a carrier control and are ± range ($n = 2$). *B*, inactivation of aconitase by RET. Mitochondria were incubated with succinate ± rotenone for 5 min. Data were normalized to a no incubation control and are ± S.E. ($n = 5$). *; $p < 0.05$ two-tailed Student's *t* test. With RET, 1.03 ± 0.08 nmol of $H_2O_2 \times min^{-1} \times$ mg of protein^{-1}; without RET, 0.13 ± 0.01 nmol of $H_2O_2 \times min^{-1} \times$ mg of protein^{-1}.

that both could be affected simultaneously by mitochondrial ROS and thereby be part of a coordinated redox regulatory pathway.

DISCUSSION

Mitochondria generate $O_2^{\cdot-}$ and H_2O_2 as byproducts of oxidative phosphorylation, and consequently, feedback regulation of mitochondrial function by these ROS is appealing. This work shows that exposure of mitochondria and cells to H_2O_2 causes one to two of the cysteine thiols of PDHK2 to become reversibly oxidized (Figs. 1 and 3). Analysis of PDHK2 mutants lacking either Cys-45 or Cys-392 indicated that these are the two redox active cysteines (Fig. 3). Higher ROS levels led to an intermolecular disulfide between two Cys-392 residues (Fig. 4). The low concentrations of H_2O_2 that modified PDHK2 did not cause bulk changes to protein thiols and GSH, but did result in oxidation of thioredoxin 2 and peroxiredoxin III (supplemental Fig. S3). Consequently, H_2O_2 may react directly with PDHK2 to form a sulfenic acid, or may oxidize other thiol redox couples, which then modify PDHK2 by thiol disulfide exchange. H_2O_2 concentration inversely correlates with PDHK2 activity (Figs. 2 and 4) and directly correlates with flux through PDC (Fig. 5). Furthermore, mutation of either Cys-45 or Cys-392 on PDHK2 to alanine changes the phosphorylation profile and flux through PDC in the presence of H_2O_2 (Figs. 4 and 5). These results suggest that $O_2^{\cdot-}$ generated by the respiratory chain dismutates to H_2O_2 that induces thiol modifications on PDHK2, and these inhibit PDC phosphorylation and increase mitochondrial respiration.

PDHK2 is a noncovalent dimer *in vivo* that transitions from an inactive dimer with disordered C-terminal tails to a weakly active dimer with partially ordered C-terminal tails (19, 23, 24). This creates a binding site for the L2 domain of PDC, leading to complete ordering of the C-terminal tails and full kinase activity on binding to its PDC substrate (Fig. 7*A*) (24, 25). Cys-392 is located on the flexible C-terminal tail of PDHK2 next to a conserved DW-motif that is required for partial ordering of the C-terminal tails (Fig. 7*A*) (26). Oxidative modification of Cys-392 could prevent formation of the L2 binding site, whereas the C392A mutation could allow association of PDHK2 with L2 even under oxidizing conditions (Fig. 4*A*). PDHK2 formed a covalent dimer when exposed to ROS, and this was not detected in the C392A mutant (Fig. 4*C*). The C-terminal tails are not resolved in the inactive structure, but a disulfide cross-link between Cys-392 residues (Fig. 4*C* and supplemental Fig. S8) could hold PDHK2 in an inactive state. How Cys-45 affects PDHK2 activity is clearly more complicated and at this stage uncertain. PDHK2 activity is inhibited by the substrates of PDC (pyruvate, NAD^+, and CoA) and stimulated by L2 and the products of PDC (NADH and acetyl-CoA), but only pyruvate has an allosteric binding site. The effects of NAD^+/NADH and CoA/acetyl-CoA are thought to be mediated via oxidation, reduction, and acetylation of the two thiols of the lipoyl group of L2 (27). When PDHK2 binds L2, the nearest features to Cys-45 are the end of the fully ordered C-terminal tail and the lipoyl thiols (Fig. 7*A*). The requirement of the Cys-45 thiol for full PDHK2 activity (Figs. 4 and 5) could suggest that activation by NADH, acetyl-CoA, or L2 binding has been lost.

Inactivation of PDHK2 by ROS increases flux through the PDC and substrate supply to the respiratory chain, potentially favoring ROS generation (1). One possible solution to this damaging feed-forward loop is the sensitivity of aconitase to inactivation by $O_2^{\cdot-}$ (22). Inactivation of aconitase would be expected to slow the TCA cycle, limiting the increase in supply of substrates to the respiratory chain resulting from PDHK2 inactivation and thus preventing excessive and prolonged oxidative stress (Fig. 7*B*). That the same ROS signal originating from complex I by RET inactivates both PDHK2 and aconitase (Figs. 1*D* and 6*B*) is consistent with this hypothesis. In the original screen that identified PDHK2, almost all of the other mitochondrial proteins that had thiols sensitive to RET were involved in generating acetyl-CoA from fat (carnitine acetyl transferase, very long-chain acyl-CoA dehydrogenase, mitochondrial trifunctional protein, mitochondrial short-chain enoyl-CoA hydratase, and propionyl-CoA carboxylase) (3). An area for future investigation is whether excess substrate supply to mitochondria coupled with low ATP demand (1) inactivates PDHK2, aconitase, and a number of fatty acid metabolizing enzymes, and whether in some tissues, this inhibits β-oxidation and creates an excess of citrate that can be exported for fatty acid synthesis in the cytoplasm (28). Such a mechanism might shift the balance between carbohydrate and fat metabolism and help explain why the extreme sensitivity of aconitase to $O_2^{\cdot-}$ has not been eliminated by evolution (22), why homozygous manganese superoxide dismutase knock-out mice are hypothermic, accumulate fat, and die within a week of birth (29), why heterozygous manganese superoxide dismutase knock-out mice are insulin-resistant (30), and why mitochondria-targeted antioxidants lower fat content and protect against insulin resistance (30, 31).

To conclude, here we have shown that PDK2, one of the key regulators of carbohydrate entry into the TCA cycle, is redox-regulated and that identical low levels of ROS can also inactivate aconitase. These findings suggest that pathways may exist through which the production of $O_2^{\cdot-}$ and H_2O_2 by the respiratory chain may act as redox signals to modulate carbohydrate metabolism.

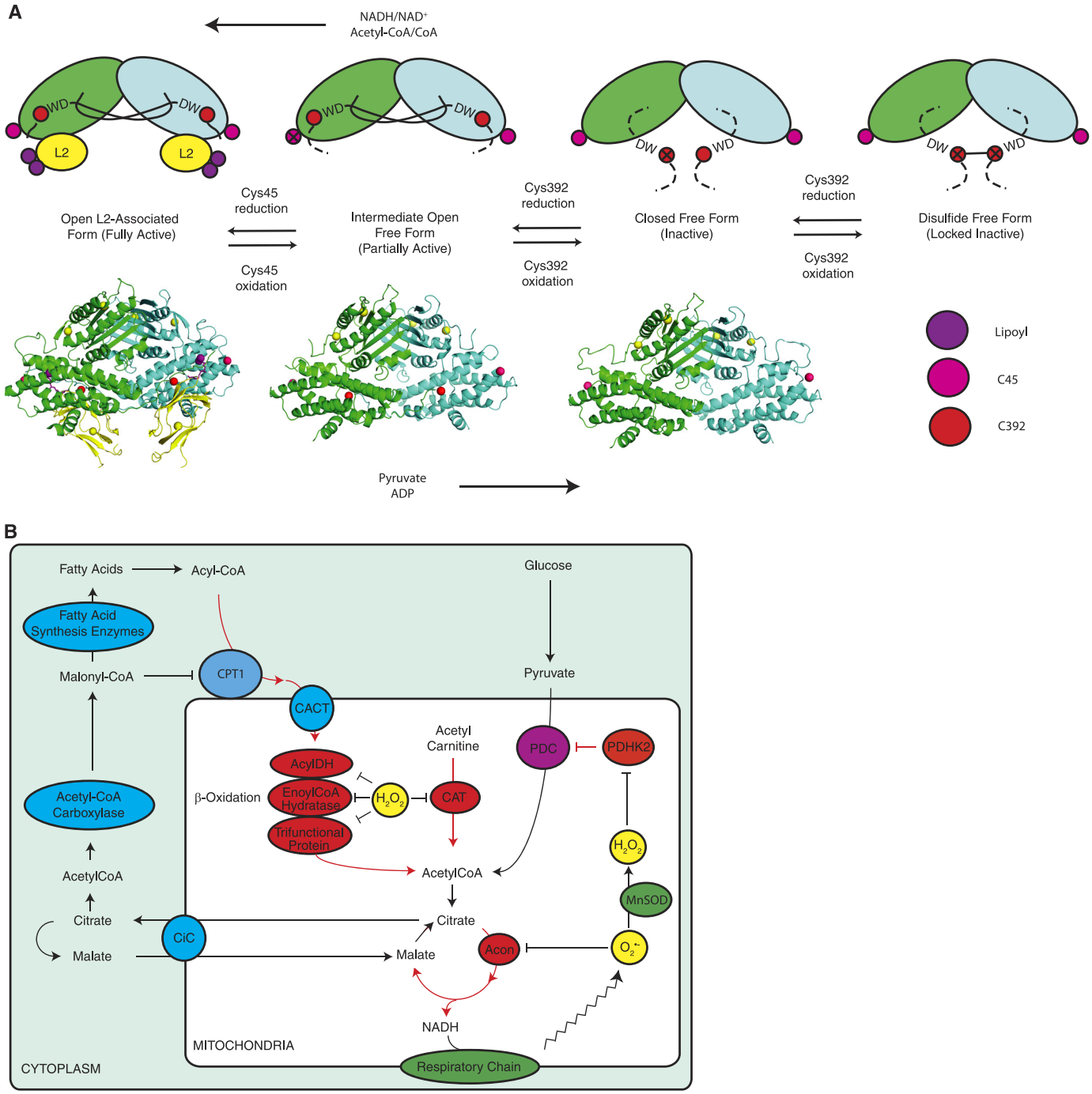

FIGURE 7. **Possible models for PDHK2 redox regulation at molecular and metabolic levels.** *A*, a model for redox regulation of PDHK2. Cys-45 (*pink*) and Cys-392 (*red*) of PDHK2 (*blue* and *green*) are reduced within cells favoring association with the L2 domain of PDC (*yellow*) forming a fully active kinase. Cys-45 is near the two lipoyl thiols (*purple*) on L2 and near the end of the C-terminal tail (*completely solid line*) when it is ordered (3CRL). Cys-45 oxidation may decrease PDHK2 activity by limiting association with L2 or preventing activation by NADH and acetyl-CoA. A reduced Cys-392 is likely to be required for initial ordering of the C-terminal tail (*solid* and *dashed line*) to form a partially active free enzyme (2BTZ). Oxidation of Cys-392 could completely disorder the C-terminal tail (*completely dashed line*), resulting in inactive PDHK2 in which Cys-392 is not resolved (2BU8). Further oxidation of Cys-392 to a disulfide could lock PDHK2 in an inactive state. Cys-45 and Cys-392 are closer to known regulatory features of PDHK2, the lipoyl thiols and the C-terminal tail, than other cysteine thiols on L2 or PDHK2 (*yellow spheres*). *B*, a model where inactivation of PDHK2 and aconitase (*Acon*) ROS could shift metabolism toward fatty acid synthesis. In this model, PDC converts pyruvate to acetyl-CoA that enters the TCA cycle, forming citrate. The NADH/NAD^+ ratio rises as NADH generation exceeds ATP demand. This leads to O_2^- generation that inactivates aconitase and slows NADH formation, limiting ROS exposure. This O_2^- is also converted to H_2O_2 by manganese superoxide dismutase, slowing β-oxidation and inactivating PDHK2. This favors generation of acetyl-CoA from carbohydrates. PDC activation and aconitase inactivation causes citrate to be exported to the cytoplasm via the citrate carrier (*CiC*) for fatty acid synthesis. As NADH is only generated by PDC and malate dehydrogenase, increased fluxes through PDC can occur without increased ATP demand, allowing rapid conversion of carbohydrates to fat. As manganese superoxide dismutase protects aconitase, but not PDHK2, from inactivation, it could have a critical regulatory role in fat deposition. *Red*, pathways and enzymes inactivated by ROS. *Purple*, enzymes activated in a high ROS environment. *CPT1*, carnitine palmitoyltransferase 1; *CACT*, carnitine:acylcarnitine translocase; *CAT*, carnitine acetyltransferase; *MnSOD*, manganese superoxide dismutase.

REFERENCES

1. Murphy, M. P. (2009) How mitochondria produce reactive oxygen species. *Biochem. J.* **417,** 1–13
2. Janssen-Heininger, Y. M., Mossman, B. T., Heintz, N. H., Forman, H. J., Kalyanaraman, B., Finkel, T., Stamler, J. S., Rhee, S. G., and van der Vliet, A. (2008) Redox-based regulation of signal transduction: principles, pitfalls, and promises. *Free Radic. Biol. Med.* **45,** 1–17
3. Hurd, T. R., Prime, T. A., Harbour, M. E., Lilley, K. S., and Murphy, M. P. (2007) Detection of reactive oxygen species-sensitive thiol proteins by redox difference gel electrophoresis: implications for mitochondrial redox signaling. *J. Biol. Chem.* **282,** 22040–22051
4. Rhee, S. G. (2006) Cell signaling. H2O2, a necessary evil for cell signaling. *Science* **312,** 1882–1883
5. D'Autréaux, B., and Toledano, M. B. (2007) ROS as signaling molecules: mechanisms that generate specificity in ROS homeostasis. *Nat. Rev. Mol. Cell Biol.* **8,** 813–824
6. Sundaresan, M., Yu, Z. X., Ferrans, V. J., Irani, K., and Finkel, T. (1995) Requirement for generation of H_2O_2 for platelet-derived growth factor signal transduction. *Science* **270,** 296–299
7. Veal, E. A., Day, A. M., and Morgan, B. A. (2007) Hydrogen peroxide sensing and signaling. *Mol. Cell* **26,** 1–14
8. Patel, M. S., and Korotchkina, L. G. (2006) Regulation of the pyruvate dehydrogenase complex. *Biochem. Soc. Trans.* **34,** 217–222
9. Randle, P. J. (1995) Metabolic fuel selection: general integration at the whole-body level. *Proc. Nutr. Soc.* **54,** 317–327
10. Yeaman, S. J., Hutcheson, E. T., Roche, T. E., Pettit, F. H., Brown, J. R., Reed, L. J., Watson, D. C., and Dixon, G. H. (1978) Sites of phosphorylation on pyruvate dehydrogenase from bovine kidney and heart. *Biochemistry* **17,** 2364–2370
11. Roche, T. E., Baker, J. C., Yan, X., Hiromasa, Y., Gong, X., Peng, T., Dong, J., Turkan, A., and Kasten, S. A. (2001) Distinct regulatory properties of pyruvate dehydrogenase kinase and phosphatase isoforms. *Prog. Nucleic Acid Res. Mol. Biol.* **70,** 33–75
12. Bowker-Kinley, M. M., Davis, W. I., Wu, P., Harris, R. A., and Popov, K. M. (1998) Evidence for existence of tissue-specific regulation of the mammalian pyruvate dehydrogenase complex. *Biochem. J.* **329,** 191–196
13. Makmura, L., Hamann, M., Areopagita, A., Furuta, S., Muñoz, A., and Momand, J. (2001) Development of a sensitive assay to detect reversibly oxidized protein cysteine sulfhydryl groups. *Antioxid. Redox Signal.* **3,** 1105–1118
14. Rardin, M. J., Wiley, S. E., Naviaux, R. K., Murphy, A. N., and Dixon, J. E. (2009) Monitoring phosphorylation of the pyruvate dehydrogenase complex. *Anal. Biochem.* **389,** 157–164
15. Cochemé, H. M., and Murphy, M. P. (2008) Complex I is the major site of mitochondrial superoxide production by paraquat. *J. Biol. Chem.* **283,** 1786–1798
16. Thor, H., Smith, M. T., Hartzell, P., Bellomo, G., Jewell, S. A., and Orrenius, S. (1982) The metabolism of menadione (2-methyl-1,4-naphthoquinone) by isolated hepatocytes: a study of the implications of oxidative stress in intact cells. *J. Biol. Chem.* **257,** 12419–12425
17. Cox, A. G., Pullar, J. M., Hughes, G., Ledgerwood, E. C., and Hampton, M. B. (2008) Oxidation of mitochondrial peroxiredoxin 3 during the initiation of receptor-mediated apoptosis. *Free Radic. Biol. Med.* **44,** 1001–1009
18. Popp, D. A., Kiechle, F. L., Kotagal, N., and Jarett, L. (1980) Insulin stimulation of pyruvate dehydrogenase in an isolated plasma membrane-mitochondrial mixture occurs by activation of pyruvate dehydrogenase phosphatase. *J. Biol. Chem.* **255,** 7540–7543
19. Knoechel, T. R., Tucker, A. D., Robinson, C. M., Phillips, C., Taylor, W., Bungay, P. J., Kasten, S. A., Roche, T. E., and Brown, D. G. (2006) Regulatory roles of the N-terminal domain based on crystal structures of human pyruvate dehydrogenase kinase 2 containing physiological and synthetic ligands. *Biochemistry* **45,** 402–415
20. Whitehouse, S., Cooper, R. H., and Randle, P. J. (1974) Mechanism of activation of pyruvate dehydrogenase by dichloroacetate and other halogenated carboxylic acids. *Biochem. J.* **141,** 761–774
21. Popov, K. M., Kedishvili, N. Y., Zhao, Y., Gudi, R., and Harris, R. A. (1994) Molecular cloning of the p45 subunit of pyruvate dehydrogenase kinase. *J. Biol. Chem.* **269,** 29720–29724
22. Hausladen, A., and Fridovich, I. (1994) Superoxide and peroxynitrite inactivate aconitases, but nitric oxide does not. *J. Biol. Chem.* **269,** 29405–29408
23. Green, T., Grigorian, A., Klyuyeva, A., Tuganova, A., Luo, M., and Popov, K. M. (2008) Structural and functional insights into the molecular mechanisms responsible for the regulation of pyruvate dehydrogenase kinase 2. *J. Biol. Chem.* **283,** 15789–15798
24. Kato, M., Chuang, J. L., Tso, S. C., Wynn, R. M., and Chuang, D. T. (2005) Crystal structure of pyruvate dehydrogenase kinase 3 bound to lipoyl domain 2 of human pyruvate dehydrogenase complex. *EMBO J.* **24,** 1763–1774
25. Wynn, R. M., Kato, M., Chuang, J. L., Tso, S. C., Li, J., and Chuang, D. T. (2008) Pyruvate dehydrogenase kinase-4 structures reveal a metastable open conformation fostering robust core-free basal activity. *J. Biol. Chem.* **283,** 25305–25315
26. Li, J., Kato, M., and Chuang, D. T. (2009) Pivotal role of the C-terminal DW-motif in mediating inhibition of pyruvate dehydrogenase kinase 2 by dichloroacetate. *J. Biol. Chem.* **284,** 34458–34467
27. Steussy, C. N., Popov, K. M., Bowker-Kinley, M. M., Sloan, R. B., Jr., Harris, R. A., and Hamilton, J. A. (2001) Structure of pyruvate dehydrogenase kinase: novel folding pattern for a serine protein kinase. *J. Biol. Chem.* **276,** 37443–37450
28. James, A. M., Collins, Y., Logan, A., and Murphy, M. P. (2012) Mitochondrial oxidative stress and the metabolic syndrome. *Trends Endocrinol. Metab.* **23,** 429–434
29. Li, Y., Huang, T. T., Carlson, E. J., Melov, S., Ursell, P. C., Olson, J. L., Noble, L. J., Yoshimura, M. P., Berger, C., Chan, P. H., Wallace, D. C., and Epstein, C. J. (1995) Dilated cardiomyopathy and neonatal lethality in mutant mice lacking manganese superoxide dismutase. *Nat. Genet.* **11,** 376–381
30. Hoehn, K. L., Salmon, A. B., Hohnen-Behrens, C., Turner, N., Hoy, A. J., Maghzal, G. J., Stocker, R., Van Remmen, H., Kraegen, E. W., Cooney, G. J., Richardson, A. R., and James, D. E. (2009) Insulin resistance is a cellular antioxidant defense mechanism. *Proc. Natl. Acad. Sci. U.S.A.* **106,** 17787–17792
31. Rodriguez-Cuenca, S., Cochemé, H. M., Logan, A., Abakumova, I., Prime, T. A., Rose, C., Vidal-Puig, A., Smith, A. C., Rubinsztein, D. C., Fearnley, I. M., Jones, B. A., Pope, S., Heales, S. J., Lam, B. Y., Neogi, S. G., McFarlane, I., James, A. M., Smith, R. A., and Murphy, M. P. (2010) Consequences of long-term oral administration of the mitochondria-targeted antioxidant MitoQ to wild-type mice. *Free Radic. Biol. Med.* **48,** 161–172